Factors Influencing the Thermodynamics of Zinc Alkoxide Formation by Alcoholysis of the Terminal Hydroxide Complex, [Tp$^{Bu^t,Me}$]ZnOH: An Experimental and Theoretical Study Relevant to the Mechanism of Action of Liver Alcohol Dehydrogenase

Catherine Bergquist, Hannah Storrie, Lawrence Koutcher, Brian M. Bridgewater, Richard A. Friesner,* and Gerard Parkin*

Contribution from the Department of Chemistry, Columbia University, New York, New York 10027

Received June 26, 2000

Abstract: The factors that influence the formation of a tetrahedral alkoxide complex related to a critical intermediate of the catalytic cycle of liver alcohol dehydrogenase have been probed by a combined experimental and computational investigation of the reactions of the tris(pyrazolyl)hydroborato zinc hydroxide complexes [Tp$^{RR'}$]ZnOH with alcohols. The study demonstrates that zinc alkoxide formation is electronically favored by incorporation of electron-withdrawing substituents in the alcohol but is sterically disfavored for bulky alkoxides. A computational analysis indicates that these trends are a result of homolytic Zn−OR and Zn−OAr BDEs being more sensitive to the nature of R and Ar than are the corresponding H−OR and H−OAr BDEs. Thus, electron-withdrawing substituents increase Zn−OAr bond energies to a greater extent than H−OAr bond energies, while bulky substituents decrease Zn−OR bond energies to a greater extent than H−OR bond energies. With the exception of derivatives of acidic alcohols (e.g., nitrophenol), the zinc alkoxide complexes [Tp$^{RR'}$]-ZnOR are very unstable toward hydrolysis. This hydrolytic instability of simple zinc alkoxide complexes suggests that the active site environment of LADH plays an important role in stabilizing the alkoxide intermediate, possibly via hydrogen-bonding interactions.

Introduction

Zinc alkoxide species are proposed to be essential intermediates in the oxidation of alcohols catalyzed by liver alcohol dehydrogenase (LADH).[1−3] Such species are generated by displacement of the water molecule at the tetrahedral active site, accompanied by proton transfer (Scheme 1). An understanding of the factors that influence the stability of tetrahedral zinc alkoxide complexes with respect to hydrolysis is, therefore, critical to understanding the mechanism of action of LADH. In this paper, we report a combined experimental and computational study to quantify the effect of varying the alkoxide group on equilibria involving alcoholysis of a tetrahedral zinc hydroxide complex. Specifically, the results demonstrate that incorporation of electron-withdrawing substituents promotes the formation of a tetrahedral alkoxide species.

(1) (a) Holm, R. H.; Kennepohl, P.; Solomon, E. I. *Chem. Rev.* **1996**, *96*, 2239−2314. (b) Lipscomb, W. N.; Sträter, N. *Chem. Rev.* **1996**, *96*, 2375−2433. (c) Kimura, E.; Koike, T.; Shionoya, M. *Struct. Bond.* **1997**, *89*, 1−28.

(2) For studies modeling aspects of LADH structure and chemistry, see: (a) Bergquist, C.; Parkin, G. *Inorg. Chem.* **1999**, *38*, 422−423. (b) Kimblin, C.; Hascall, T.; Parkin, G. *Inorg. Chem.* **1997**, *36*, 5680−5681. (c) Shoner, S. C.; Humphreys, K. J.; Barnhart, D.; Kovacs, J. A. *Inorg. Chem.* **1995**, *34*, 5933−5934. (d) Kimura, E.; Shionoya, M.; Hoshino, A.; Ikeda, T.; Yamada, Y. *J. Am. Chem. Soc.* **1992**, *114*, 10134−10137. (e) Engbersen, J. F. J.; Koudijs, A.; van der Plas, H. C. *J. Org. Chem.* **1990**, *55*, 3647−3654. (f) Kellogg, R. M.; Hof, R. P. *J. Chem. Soc., Perkin Trans. 1* **1996**, 1651−1657. (g) Müller, B.; Schneider, A.; Tesmer, M.; Vahrenkamp, H. *Inorg. Chem.* **1999**, *38*, 1900−1907.

(3) For computational studies concerned with LADH structure and mechanism, see: (a) Ryde, U. *Int. J. Quantum Chem.* **1994**, *52*, 1229−1243. (b) Ryde, U. *J. Comput. Aid. Mol. Des.* **1996**, *10*, 153−164. (c) Cini, R. *J. Biomol. Struct. Dyn.* **1999**, *16*, 1225−1237. (d) Ryde, U. *Eur. Biophys. J.* **1996**, *24*, 213−221. (e) Agarwal, P. K.; Webb, S. P.; Hammes-Schiffer, S. *J. Am. Chem. Soc.* **2000**, *122*, 4803−4812.

Scheme 1

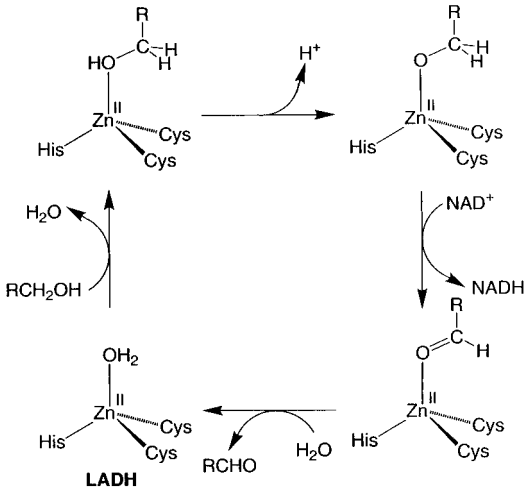

Results and Discussion

The active site of LADH is composed of a tetrahedral zinc center which is attached to the protein backbone by the nitrogen and sulfur donors of one histidine and two cysteine residues (Scheme 1). Synthetic analogues with this coordination environment that also feature the catalytically important aqua (or hydroxide) entity are, however, unknown.[2b] Furthermore, regardless of the nature of the supporting ligands, the formation of mononuclear tetrahedral zinc alkoxide complexes from zinc hydroxide derivatives is not well documented. Two notable examples, however, are (i) the synthesis of alkoxide complexes by the reactions of tris(pyrazolyl)hydroborato zinc hydroxide

10.1021/ja002286d CCC: $19.00
Published on Web 12/02/2000

Scheme 2

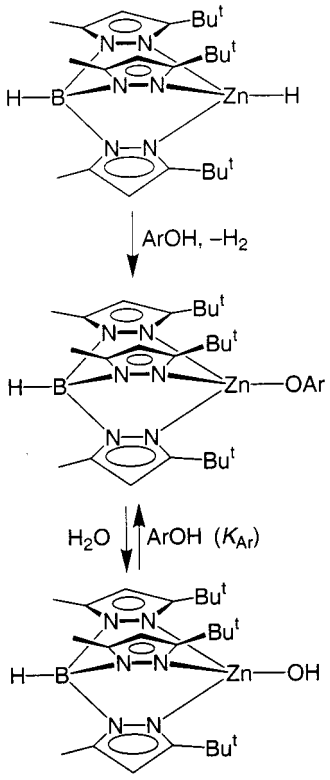

derivatives [Tp$^{RR'}$]ZnOH with ROH,[2a,4] and (ii) the intramolecular generation of alkoxide complexes in which the alcohol functionality is pendant to the macrocyclic ligand that binds the zinc.[5]

Since mononuclear zinc hydroxide complexes with a [SSN]-ZnOH composition are unknown, we have selected [Tp$^{Bu^t,Me}$]-ZnOH for studies designed to evaluate the factors responsible for influencing alcoholysis equilibria, recognizing that the coordination motif is not identical to that of LADH. We have previously reported that the equilibrium constants for the formation of the alkoxide complexes [Tp$^{Bu^t,Me}$]ZnOR from [Tp$^{Bu^t,Me}$]ZnOH and ROH (R = Me, Et, Pr^i, Bu^t) are highly dependent upon the nature of R, decreasing markedly in the following sequence: Me > Et > Pr^i > Bu^t.[2a] Since this trend is presumably the result of a composite steric and electronic influence, we have sought to separate these components by studying a series of para-substituted phenols, *p*-XC_6H_4OH, for which electronic substituent parameters (e.g., Hammett σ constants) are available.

[Tp$^{Bu^t,Me}$]ZnOH reacts with a variety of *p*-XC_6H_4OH derivatives to give the phenoxide complexes [Tp$^{Bu^t,Me}$]ZnOC_6H_4X as components in an equilibrium mixture. The latter complexes may be independently synthesized by the irreversible reactions of the hydride complex [Tp$^{Bu^t,Me}$]ZnH with *p*-XC_6H_4OH (Scheme 2). The molecular structures of [Tp$^{Bu^t,Me}$]ZnOC_6H_4X (X = Bu^t, C(O)Me, NH_2, NO_2) have been determined by X-ray diffraction, thereby confirming their mononuclear nature, as illustrated for [Tp$^{Bu^t,Me}$]Zn$OC_6H_4NO_2$ in Figure 1. Selected bond lengths and angles for the [Tp$^{Bu^t,Me}$]ZnOC_6H_4X derivatives are summarized in Table 1.

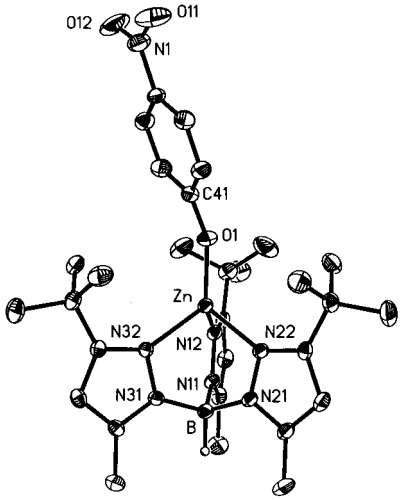

Figure 1. Molecular structure of [Tp$^{Bu^t,Me}$]Zn$OC_6H_4NO_2$.

The equilibrium constants (K_{Ar}) for the alcoholysis reactions of [Tp$^{Bu^t,Me}$]ZnOH with *p*-XC_6H_4OH (Scheme 2) have been determined by ^{1}H NMR spectroscopy. For the reaction with *p*-MeC_6H_4OH, the equilibrium constant in THF-d_8 was determined directly, but for all other derivatives, the equilibrium constants were obtained via a thermodynamic cycle involving the experimentally determined equilibrium constant for alkoxide exchange between [Tp$^{Bu^t,Me}$]ZnOC_6H_4Me and *p*-XC_6H_4OH. The equilibrium constant data are listed in Table 2.

A Hammett plot[6] of log *K* versus σ gives a good linear correlation with a ρ value of 2.8 (Figure 2), indicating that zinc aryloxide formation is strongly favored by electron-withdrawing substituents.[7] For comparison, the equilibrium is substantially more sensitive to electronic effects than is the exchange of (Me_2C_2)Re(O)(OPh) with ArOH, which is characterized by a ρ value of only 0.71 for a plot of log *K* versus σ.[8] To gain more insight into the factors influencing the formation of the aryloxide complexes, we have studied the thermodynamics of the alcoholysis reactions using computational methods.

Significantly, DFT calculations (B3LYP) performed using Jaguar[9] are in excellent agreement with the experimental results. Thus, the calculated electronic energy differences are only ~2.5 kcal mol^{-1} less exothermic than the experimental enthalpy changes (Table 2). More importantly than the difference being small, it is also roughly constant throughout the series, such that the correlation between the experimental and calculated results is excellent (Figure 3).

The effect of a substituent on the energetics of the reactions between [Tp$^{Bu^t,Me}$]ZnOH and ArOH is dictated by its influence on the respective [Tp$^{Bu^t,Me}$]Zn−OAr and H−OAr BDEs. In this regard, the thermodynamic cycle illustrated in Scheme 3 demonstrates that the substituent effect can be conceptually discussed equally well in terms of the influence of substituents on either homolytic or heterolytic [Tp$^{Bu^t,Me}$]Zn−OAr and H−OAr BDEs.[10] However, since homolytic ArO−H BDEs have been discussed to a greater extent in the literature,[11] and also the effect of solvation on homolytic BDEs is less than that on heterolytic BDEs, it is more useful to focus attention on the effects of the alcoholysis reactions in terms of homolytic BDEs.

The experimental and computational studies indicate that electron-withdrawing substituents favor the formation of the zinc

(4) Walz, R.; Weis, K.; Ruf, M.; Vahrenkamp, H. *Chem. Ber./Recl.* **1997**, *130*, 975−980.

(5) (a) Kimura, E.; Kodama, Y.; Koike, T.; Shiro, M. *J. Am. Chem. Soc.* **1995**, *117*, 8304−8311. (b) Kimura, E.; Nakamura, I.; Koike, T.; Shionoya, M.; Kodama, Y.; Ikeda, T.; Shiro, M. *J. Am. Chem. Soc.* **1994**, *116*, 4764−4771. (c) Koike, T.; Kajitani, S.; Nakamura, I.; Kimura, E.; Shiro, M. *J. Am. Chem. Soc.* **1995**, *117*, 1210−1219.

(6) Hansch, C.; Leo, A.; Taft, R. W. *Chem. Rev.* **1991**, *91*, 165−195.

(7) A plot based on σ^- has a slope of 2.0.

(8) Erikson, T. K. G.; Bryan, J. C.; Mayer, J. M. *Organometallics* **1988**, *7*, 1930−1938.

(9) Jaguar 3.5 and 4.0, Schrödinger, Inc., Portland, OR, 1998.

Table 1. Selected Bond Lengths and Angles

	$[Tp^{Bu^t,Me}]ZnOC_6H_4C(O)Me$	$[Tp^{Bu^t,Me}]ZnOC_6H_4NO_2$	$[Tp^{Bu^t,Me}]ZnOC_6H_4NH_2$	$[Tp^{Bu^t,Me}]ZnOC_6H_4Bu^t$
$Zn-N_{av}$/Å	2.04	2.04	2.05	2.05
Zn−O/Å	1.827(2)	1.849(3)	1.845(2), 1.849(2)[a]	1.846(2), 1.842(2)[a]
Zn−O−C/deg	168.4(2)	157.5(3)	146.6(2), 147.5(3)[a]	145.0(2), 152.7(2)[a]

[a] Data for two crystallographically independent molecules.

Table 2. Equilibrium Constant and Enthalpy Data for Alcoholysis Reactions of $[Tp^{Bu^t,Me}]ZnOH$

ROH	K (300 K)	ΔH_{expt}/ kcal mol^{-1} [a]	ΔE_{calc}/ kcal mol^{-1}
Bu^t [b]	$\sim 10^{-8}$	~8	8.86
Pr^i [b]	$3(1) \times 10^{-5}$	3.5(2)	7.14
Et[b]	$9(2) \times 10^{-4}$	1.5(2)	4.37
Me[b]	$1.4(2) \times 10^{-3}$	1.2(1)	4.03
C_6H_4OMe	4.2(9)	−0.9(1)	1.47
$C_6H_4Bu^t$	4.8(10)	−0.9(1)	1.06
C_6H_4Me	4.9(10)	−1.0(1)	1.64
C_6H_5	$1.0(2) \times 10^1$	−1.4(1)	1.17
C_6H_4I	$9(2) \times 10^1$	−2.7(1)	−0.44
$C_6H_4CO_2Me$	$2.7(6) \times 10^2$	−3.3(1)	−1.04
C_6H_4COMe	$3.1(6) \times 10^2$	−3.4(1)	−1.42
$C_6H_4NO_2$	$3.5(8) \times 10^3$	−4.9(1)	−3.57

[a] ΔH values are calculated by assuming values of −9 eu for reactions involving ROH and 0 eu for reactions involving ArOH. These values are based on measured values for the reactions between (i) $[Tp^{Bu^t,Me}]ZnOH$ and MeOH in MeOH solvent and (ii) $[Tp^{Bu^t,Me}]ZnOH$ and *p*-MeC_6H_4OH in THF. [b] Data taken from ref 2a.

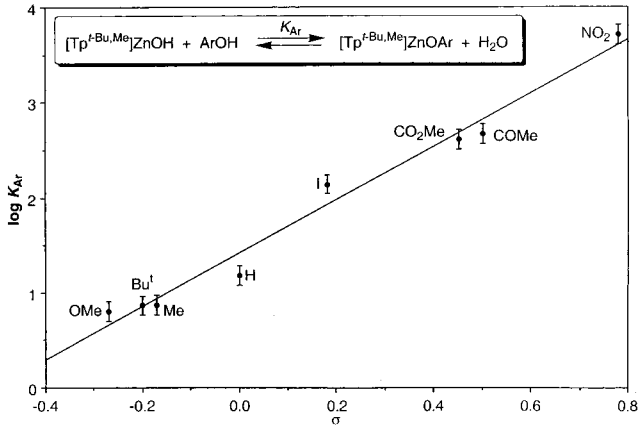

Figure 2. Hammett plot of log K versus σ for the reaction of $[Tp^{Bu^t,Me}]$-ZnOH with XC_6H_4OH.

aryloxide compound because they increase the homolytic Zn−OAr BDEs in $[Tp^{Bu^t,Me}]ZnOAr$ to a greater extent than the corresponding H−OAr BDEs.[11,12] Thus, rather than exhibiting the 1:1 correlation between M−X and H−X bond energies that has been reported for certain other systems,[13] the Zn−OAr BDE is substantially more sensitive to the para substituent than is the H−OAr BDE, by a factor of 1.4:1 (Figure 4).[14]

Previous studies indicate that electron-withdrawing para substituents increase homolytic ArO−H BDEs as a result of preferential stabilization[15] of ArOH due to increased delocalization of the electron density from the oxygen atom; destabilization of the product radical ArO• by electron-withdrawing substituents serves to reinforce this effect (Figure 5).[11,12,16] Electron-donating para substituents correspondingly decrease the H−OAr BDE, but the effect is principally due to stabilization

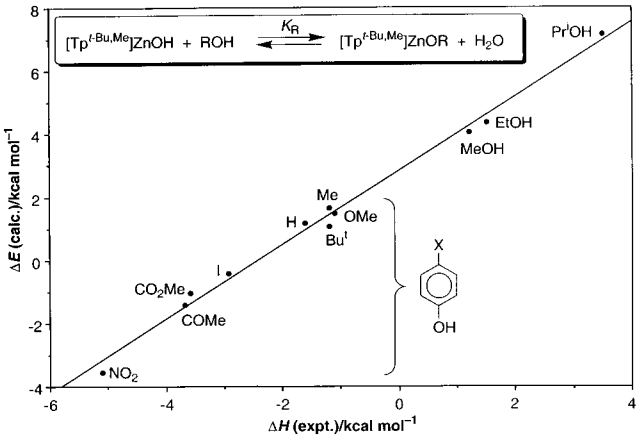

Figure 3. Correlation of experimental ΔH and calculated ΔE values for the various alcoholysis equilibria.

Scheme 3

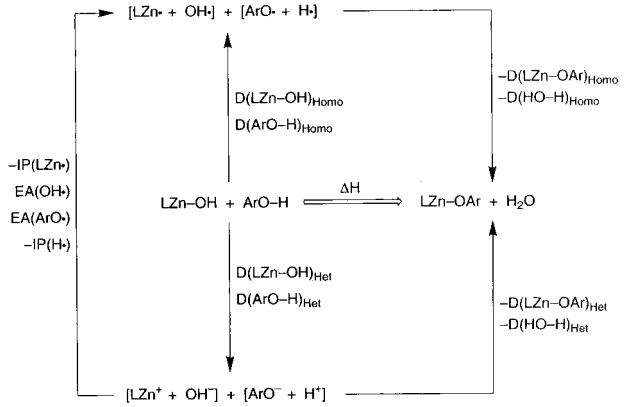

(10) Heterolytic M−OAr values are related to the homolytic values by the electron affinity of ArO• and the ionization potential of M• (M = H, $[Tp^{Bu^t,Me}]Zn$); i.e., $D(M-OAr)_{Het} = D(M-OAr)Homo - EA(OAr^•) + IP(M^•)$.

(11) For a recent review of homolytic ArO−H BDEs, see: Borges dos Santos, R. M.; Martinho Simões, J. A. *J. Phys. Chem. Ref. Data* **1998**, *27*, 707−739.

(12) For other calculations on ArO−H BDEs, see: (a) Wu, Y.-D.; Lai, D. K. W. *J. Org. Chem.* **1996**, *61*, 7904−7910. (b) Brinck, T.; Haeberlein, M.; Jonsson, M. *J. Am. Chem. Soc.* **1997**, *119*, 4239−4244. (c) Bordwell, F. G.; Zhang, X.-M.; Satish, A. V.; Cheng, J.-P. *J. Am. Chem. Soc.* **1994**, *116*, 6605−6610.

(13) See, for example: (a) Bryndza, H. E.; Fong, L. K.; Paciello, R. A.; Tam, W.; Bercaw, J. E. *J. Am. Chem. Soc.* **1987**, *109*, 1444−1456. (b) Bryndza, H. E.; Tam, W. *Chem. Rev.* **1988**, *88*, 1163−1188. (c) Bryndza, H. E.; Domaille, P. J.; Tam, W.; Fong, L. K.; Paciello, R. A.; Bercaw, J. E. *Polyhedron* **1988**, *7*, 1441−1452.

(14) The data in Figure 4 correspond to the calculated values. The experimental ratio is also 1.4:1, but for two fewer compounds since data are not available. Specifically, $D(Zn-OAr) = 1.40D(H-OAr) - D(Zn-OH) - 152$ kcal mol^{-1}.

(15) It is recognized that the word "stabilization" is being used loosely in this context since it is inappropriate to compare energies of molecules with different compositions. See ref 11.

(16) For calculations on ROH, see: (a) Damrauer R. *J. Am. Chem. Soc.* **2000**, *122*, 6739−6745. (b) Safi, B.; Choho, K.; De Proft, F.; Geerlings, P. *J. Phys. Chem. A* **1998**, *102*, 5253−5259. (c) De Proft, F.; Langenaeker, W.; Geerlings, P. *Tetrahedron* **1995**, *51*, 4021−4032. (d) Tupper, K. J.; Gajewski, J. J.; Counts, R. W. *J. Mol. Struct (THEOCHEM)* **1991**, *236*, 211−217.

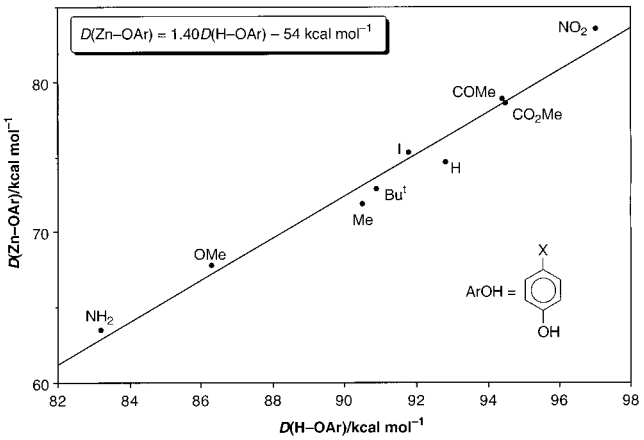

Figure 4. Correlation of calculated homolytic Zn−OAr and H−OAr BDEs.

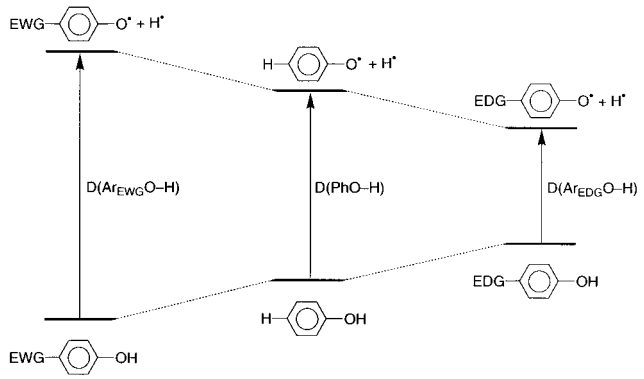

Figure 5. Conceptual influence of electron-donating and electron-withdrawing substituents on XC_6H_4O-H homolytic BDEs (see refs 11 and 12a).

of the ArO• radical, with destabilization of ArOH contributing only to a small degree.

Within the construct that rationalizes the increase in homolytic H−OAr BDE in terms of the ability of an electron-withdrawing substituent to stabilize electron density on the oxygen atom, the greater sensitivity of the Zn−OAr BDE may be attributed to the $Zn^{\delta+}-OAr^{\delta-}$ bond being more polar than the $H^{\delta+}-OAr^{\delta-}$ bond. For example, the Mulliken charges on the oxygen atom in $[Tp^{Bu^t,Me}]$ZnOAr are in the range −0.73 to −0.77, whereas those in ArOH are in the range −0.39 to −0.41. An electron-withdrawing substituent would, therefore, exert a greater influence in stabilizing the partial negative charge on the oxygen atom in $[Tp^{Bu^t,Me}]$ZnOAr than that in ArOH, with the result that the Zn−OAr BDE is more sensitive to the substituent than is the H−OAr BDE, as illustrated in Figure 6.

Alternatively, in terms of arguments based on *heterolytic* bond dissociation energies, the experimental and computational studies indicate that electron-withdrawing substituents *decrease* the heterolytic Zn−OAr bond dissociation energies to a *lesser* extent than those for the H−OAr bond energies (Table 3 and Figure 7). Essentially, electron-withdrawing substituents decrease both heterolytic Zn−OAr and H−OAr bond energies because they stabilize the ArO^- anion to a greater extent than M−OAr (M = Zn, H), but the effect is less for the Zn−OAr bond because it is more polar (i.e., the aryloxide moiety is closer to OAr^-); indeed, the heterolytic Zn−OAr BDEs are ∼200 kcal mol^{-1} lower than the corresponding heterolytic H−OAr BDEs (Table 3).

It is also important to emphasize that electron-withdrawing substituents (relative to hydrogen) create a more significant

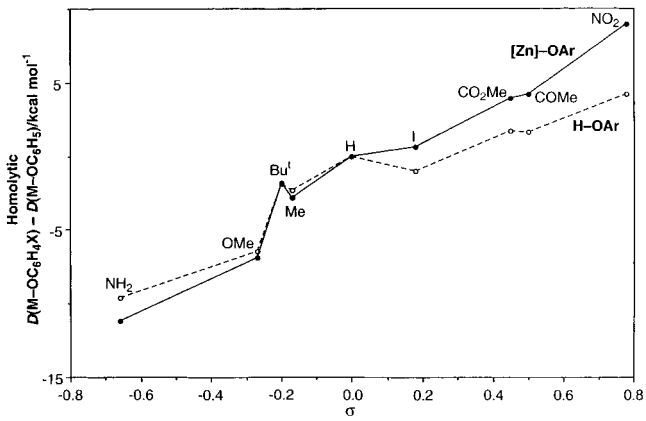

Figure 6. Variation of calculated homolytic Zn−OAr and H−OAr BDEs as a function of the σ value of the para substituent.

differential in relative Zn−OAr and H−OAr bond energies than do electron-donating substituents. Thus, electron-donating substituents (OMe, Bu^t, Me) influence both Zn−OAr and H−OAr bond energies to a similar degree (Figures 6 and 7); NH_2, the most strongly electron-donating substituent, is the only one for which a notable differential between relative Zn−OAr and H−OAr BDEs exists (Figures 6 and 7). For the homolytic bond dissociation energies, this result is in accord with the aforementioned notion that an electron-donating substituent principally modifies the H−OAr bond energy by influencing the energy of the ArO• radical as opposed to exerting a ground-state effect on ArOH.[11,12] Thus, for the extreme case that a substituent influences only the radical and not the ground state, its influence on a M−OAr BDE would be independent of the nature of M (M = Zn, H).

The above results suggest that the influence of electron-withdrawing substituents on alcoholysis equilibria is associated with preferential stabilization of the partial negative charge on the oxygen atom of $[Tp^{Bu^t,Me}]$ZnOAr as compared to that of ArOH. This interpretation is in accord with that provided by Bergman, Andersen, and Holland to rationalize the influence of electron-withdrawing substituents on equilibria involving transition metal amido, aryloxo, and alkoxo complexes.[17,18] However, the possibility that electron-withdrawing substituents increase the homolytic Zn−OAr bond dissociation energy by minimizing "filled−filled" π repulsions between the oxygen lone pairs and the electrons associated with the metal center should also be considered.[19] Bergman, Andersen, and Holland, however, invoked "Ockham's razor"[20] and concluded that if polarization effects alone may explain the data, there was no reason to incorporate "filled−filled" repulsions into the argument. In this regard, it should be noted that "filled−filled" π repulsions are clearly not possible for ArOH, but yet the H−OAr BDE is still strongly influenced by the para substituent.

Support for the proposal that the greater sensitivity of the Zn−OAr versus H−OAr bond is due to the greater polarity of the Zn−OAr bond is provided by application of the dual-parameter $E-C$ model.[21] Specifically, this model separates a substituent effect into electrostatic and covalent components via

(17) Holland, P. L.; Andersen, R. A.; Bergman, R. G. *Comments Inorg. Chem.* **1999**, *21*, 115−129.

(18) Holland, P. L.; Andersen, R. A.; Bergman, R. G.; Huang, J.; Nolan, S. P. *J. Am. Chem. Soc.* **1997**, *119*, 12800−12814.

(19) Caulton, K. G. *New. J. Chem.* **1994**, *18*, 25−41.

(20) Rodríguez-Fernández, J. L. *Endeavour* **1999**, *23*, 121−125.

(21) (a) Drago, R. S. *Applications of Electrostatic-Covalent Models in Chemistry*; Surfside Scientific Publishers: Gainesville, FL, 1994. (b) Vogel, G. C.; Drago, R. S. *J. Chem. Educ.* **1996**, *73*, 701−707. (c) Drago, R. S.; Dadmun, A. P. *J. Am. Chem. Soc.* **1993**, *115*, 8592−8602.

Table 3. Homolytic and [Heterolytic] Bond Dissociation Energies

R	D(RO−H)$_{expt}$/ kcal mol^{-1}	D(RO−H)$_{calc}$/ kcal mol^{-1}	D([Tp$^{Bu^t,Me}$]Zn−OR)$_{calc}$/ kcal mol^{-1}	D([Tp]Zn−OR)$_{calc}$/ kcal mol^{-1}
Bu^t	105.1[a] [375.9][d]	105.9 [385.6]	80.1 [149.3]	83.4 [172.7]
Pr^i	104.7[a] [376.7][d]	109.0 [389.9]	84.9 [155.3]	83.5 [174.0]
Et	104.2[a] [378.6][d]	108.1 [392.5]	86.7 [160.7]	82.8 [176.7]
Me	104.4[a] [381.7][d]	108.3 [396.8]	87.3 [165.4]	82.9 [181.0]
H	119[b] [390.7][b]	122.4 [419.8]	105.2 [192.2]	99.7 [206.7]
$C_6H_4NH_2$	79.2[c] [352.5][e]	83.2 [364.7]	63.5 [134.4]	62.3 [187.0]
C_6H_4OMe	83.5[c] [350.4][e]	86.3 [362.1]	67.8 [133.2]	66.9 [191.5]
$C_6H_4Bu^t$	87.1[c] [348.5][e]	90.9 [359.4]	72.9 [130.9]	71.8 [196.5]
C_6H_4Me	86.8[c] [350.4][e]	90.5 [360.9]	71.9 [131.8]	71.4 [196.1]
C_6H_5	88.7[c] [349.2][e]	92.8 [360.1]	74.7 [131.5]	74.2 [198.8]
C_6H_4I	88.5[c] [−]	91.8 [35.7]	75.3 [124.7]	74.7 [199.3]
$C_6H_4CO_2Me$	−[337.2][e]	94.5 [345.5]	78.6 [119.1]	78.0 [202.7]
C_6H_4COMe	90.9[c] [335.6][e]	94.4 [343.9]	78.9 [117.9]	78.6 [203.3]
$C_6H_4NO_2$	94.7[c] [327.9][e]	97.0 [334.9]	83.6 [111.0]	82.8 [207.4]

[a] McMillen, D. F.; Golden, D. M. *Ann. Rev. Phys. Chem.* **1982**, *33*, 493−532. [b] Berkowitz, J.; Ellison, G. B.; Gutman, D. *J. Phys. Chem.* **1994**, *98*, 2744−2765. [c] Reference 11. [d] Ervin, K. M.; Gronert, S.; Barlow, S. E.; Gilles, M. K.; Harrison, A. G.; Bierbaum, V. M.; DePuy, C. H.; Lineberger, W. C.; Ellison, G. B. *J. Am. Chem. Soc.* **1990**, *112*, 5750−5759. [e] Lias, S. G.; Bartmess, J. E.; Liebman, J. F.; Holmes, J. L.; Levin, R. D.; Mallard, W. G. *J. Phys. Chem. Ref. Data* **1998**, *17*, Suppl. 1.

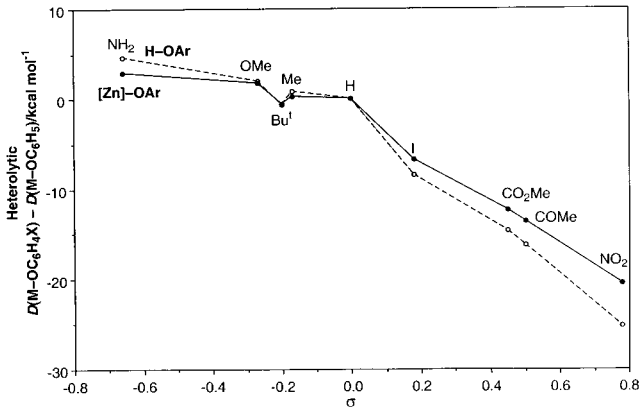

Figure 7. Variation of calculated heterlytic Zn−OAr and H−OAr BDEs as a function of the σ value of the para substituent.

the expression $\log(K_x/K_H) = d^E\Delta E^x + d^C\Delta C^x$, where ΔE^x and ΔC^x are the electrostatic and covalent substituent constants, and d^E and d^C are the electrostatic and covalent counterparts of the Hammett ρ value. The derived values, $d^E = -8.5$ and $d^C = 1.3$, indicate that the electrostatic component dominates the equilibrium and thereby suggest that electron-withdrawing substituents increase the Zn−OAr BDE to a greater extent than the H−OAr BDE (see Supporting Information) due to the greater polarity of the former bond. For comparison, the equilibrium between Cp*Ni(PEt_3)NHTol and $XC_6H_4NH_2$ is characterized by the values $d^E = -18.4$ and $d^C = 1.8$.[17,18,22]

We have also carried out calculations on the energetics of the reactions of [Tp$^{Bu^t,Me}$]ZnOH with aliphatic alcohols (MeOH, EtOH, Pr^{i}OH, Bu^{t}OH), and the results are in close agreement with the experimental results, with zinc alkoxide formation becoming increasingly disfavored in the following sequence: $K_{Me} > K_{Et} > K_{Pr^i} > K_{Bu^t}$ (see Figure 3 and Table 2).[2a] The calculations indicate that this trend is a result of the homolytic Zn−OR BDE decreasing more rapidly upon increasing the bulk of R than does the corresponding H−OR BDE (see Table 3). Presumably, the greater sensitivity of the Zn−OR BDEs is a reflection of enhanced steric interactions between R and the *tert*-butyl substituents of the [Tp$^{Bu^t,Me}$] ligand. Support for this suggestion is provided by calculations on the parent [Tp]ZnOR system, which is devoid of bulky substituents on the pyrazolyl groups. Not only do the calculations indicate that reducing the steric demands of the tris(pyrazolyl)hydroborato ligand favors the formation of the alkoxide complex (Table 4), but the calculations also indicate that the difference between the [Tp$^{Bu^t,Me}$]ZnOR and [Tp]ZnOR systems becomes more pronounced as the alkoxide group becomes bulkier (Figure 8). This trend is a consequence of the [Tp$^{Bu^t,Me}$]Zn−OR BDE decreasing more rapidly than the [Tp]Zn−OR BDE upon increasing the size of R.

Reducing the steric demands of the tris(pyrazolyl)hydroborato ligand also favors the formation of the aryloxide derivatives, but the effect is relatively insensitive to the nature of the para

(22) For the application of the dual-parameter $E-C$ model to the pK_a values of phenols, see: Bosch, E.; Rived, F.; Rosés, M.; Sales, J. *J. Chem. Soc., Perkin Trans. 2* **1999**, 1953−1958.

Table 4. Comparison of the Calculated Energetics of the Alcoholysis Reactions of [Tp$^{Bu^t,Me}$]ZnOH and [Tp]ZnOH

ROH	ΔE_{calc}\{[Tp$^{Bu^t,Me}$]Zn\}/ kcal mol^{-1}	ΔE_{calc}\{[Tp]Zn\}/ kcal mol^{-1}	$\Delta\Delta E_{calc}$/ kcal mol^{-1}
Bu^t	8.86	0.06	8.80
Pr^i	7.14	2.99	4.15
Et	4.37	2.83	1.54
Me	4.03	2.90	1.13
$C_6H_4NH_2$	2.77	−1.56	4.33
C_6H_4OMe	1.47	−3.09	4.56
$C_6H_4Bu^t$	1.06	−3.38	4.44
C_6H_4Me	1.64	−3.42	5.06
C_6H_5	1.17	−3.82	4.99
C_6H_4I	−0.44	−5.34	4.90
$C_6H_4CO_2Me$	−1.04	−5.96	4.92
C_6H_4COMe	−1.42	−6.65	5.23
$C_6H_4NO_2$	−3.57	−8.26	4.69

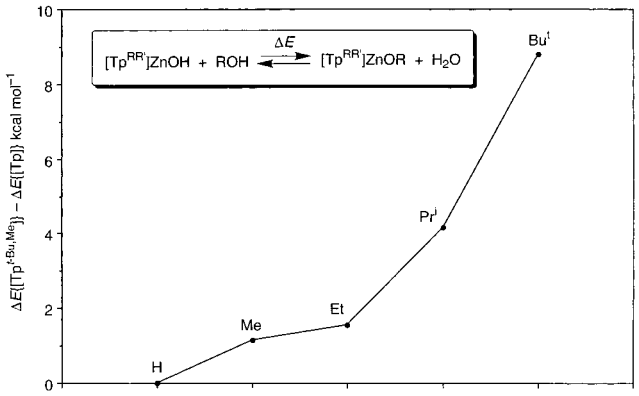

Figure 8. Influence of the tris(pyrazolyl)hydroborato ligand on the calculated energetics of the alcoholysis equilibria.

substituent. For example, $\Delta\Delta E$ for the various para-substituted aryl oxide derivatives span a range of only 0.9 kcal mol^{-1}, compared to a range of 7.7 kcal mol^{-1} for the alkoxide derivatives (Table 4).

Interestingly, while steric effects clearly play an important role in promoting the reaction of an alcohol with [Tp]ZnOH over that of [Tp$^{Bu^t,Me}$]ZnOH, it is important to note that the intrinsic *electronic* effect of the [Tp$^{Bu^t,Me}$] ligand versus the [Tp] ligand is actually to *increase* the strength of the Zn−OR bond. As an illustration for the hydroxide complexes, where steric effects are minimal, the calculated homolytic Zn−OH BDE of [Tp$^{Bu^t,Me}$]Zn−OH (105.2 kcal mol^{-1}) is greater than that of [Tp]-Zn−OH (99.7 kcal mol^{-1}); in fact, with the exception of the *tert*-butoxide derivatives, the Zn−OR BDEs of all other [Tp$^{Bu^t,Me}$]Zn−OR derivatives are greater than those of the [Tp]-Zn−OR counterparts (Table 3). The greater strength of the [Tp$^{Bu^t,Me}$]Zn−OR bonds is presumably due to the ability of the more strongly electron-donating [Tp$^{Bu^t,Me}$] ligand[23,24] to stabilize the partial positive charge on zinc to a greater degree. Increasing the steric demands of the substituent on oxygen reduces the Zn−OR BDEs of both [Tp$^{Bu^t,Me}$]Zn−OR and [Tp]Zn−OR, but since steric interactions influence the former to a greater degree, the formation of [Tp$^{Bu^t,Me}$]Zn−OR is inhibited more than that of [Tp]Zn−OR from the respective hydroxide complexes.

Recent theoretical studies have re-emphasized that alcohol deprotonation and zinc alkoxide formation takes place prior to hydride transfer to NAD$^+$; furthermore, the formation of the alkoxide is important because it facilitates the hydride-transfer step.[3e] Thus, zinc alkoxide species play a central role in the mechanism of action of LADH, with two critical issues being the kinetic and thermodynamic stability of the zinc alkoxide with respect to (a) hydrolysis and (b) hydride transfer. In this paper, we have addressed specifically the issue of the thermodynamic stability of a zinc alkoxide species with respect to hydrolysis. The study demonstrates that tetrahedral zinc alkoxides are very susceptible to hydrolysis, an observation that potentially mitigates against their viability as reactive intermediates. Nevertheless, the investigation also reveals that the stability of the zinc alkoxide complex is very sensitive to both steric and electronic influences and thereby demonstrates that the active site environment most likely plays an important role in promoting the formation of a zinc alkoxide species. For example, hydrogen bonding may provide a mechanism for stabilizing zinc alkoxide species, as illustrated by recent studies which suggest that the benzyl alkoxide ligand forms a hydrogen bond with the hydroxyl group of Ser48 in horse liver alcohol dehydrogenase.[3e,25]

Finally, it is important to emphasize that the tendency to form alkoxide compounds by alcoholysis reactions does *not* always follow the trends described in this paper (i.e., Ar > Me > Et > Pr^i > Bu^t). For example, quantitative measurements of equilibria involving (dipic)VO(OR)[26] and R′OH indicate that the alkoxides that preferentially bind to vanadium follow the opposite sequence, namely, Bu^t > Pr^i > Et > *p*-ClC$_6$H$_4$, an observation that has been rationalized in terms of the trend being dictated by the π-donor capabilities of the ligands.[27] The clear distinction between the zinc system described here and the vanadium system is that the vanadium complexes (dipic)VO(OR) are electronically unsaturated; i.e., in the absence of π-donation, the vanadium centers possess 12-electron configurations. As such, the thermodynamics for the vanadium system is strongly influenced by favorable π-donor interactions.

Experimental Section

General Considerations. All manipulations were performed using a combination of glovebox, high-vacuum, or Schlenk techniques.[28] Solvents were purified and degassed by standard procedures. NMR spectra were recorded on Bruker Avance 300wb DRX, Bruker Avance 300 DRX, Bruker Avance 400 DRX, and Bruker Avance 500 DMX spectrometers. ^{1}H and ^{13}C chemical shifts are reported in ppm relative to SiMe$_4$ ($\delta = 0$) and were referenced internally with respect to the protio solvent impurity or the ^{13}C resonances, respectively. All coupling constants are reported in hertz. IR spectra were recorded as KBr pellets on a Perkin-Elmer Spectrum 2000 spectrophotometer and are reported in reciprocal centimeters. C, H, and N elemental analyses were measured using a Perkin-Elmer 2400 CHN elemental analyzer. [Tp$^{Bu^t,Me}$]ZnH was prepared by the literature method.[2a]

Synthesis of [Tp$^{Bu^t,Me}$]ZnOC$_6$H$_4$NH$_2$. A solution of 4-aminophenol (49 mg, 0.45 mmol) and [Tp$^{Bu^t,Me}$]ZnH (200 mg, 0.41 mmol) in THF (10 mL) was heated at 120 °C for 3 days. The reaction mixture was filtered, and the volatile components were removed from the filtrate in vacuo to give [Tp$^{Bu^t,Me}$]ZnOC$_6$H$_4$NH$_2$ as a white solid (127 mg, 51%). Anal. Calcd for $C_{30}H_{46}BN_7OZn$: C, 60.4; H, 7.8; N, 16.4. Found: C, 60.7; H, 7.9; N 16.5. ^{1}H NMR (C_6D_6): 1.50 [s, 3(C(C*H*$_3$)$_3$)], 2.08 [s, 3(C*H*$_3$)], 2.73 [s, N*H*$_2$], 5.63 [s, 3(C$_3$N$_2$*H*)], 6.71 [d, $^3J_{H-H} = 9$, C$_6$*H*$_4$ (2H)], 7.20 [d, $^3J_{H-H} = 9$, C$_6$*H*$_4$ (2H)], *H*B not observed. ^{13}C NMR (C_6D_6): 12.6 [q, $^1J_{C-H} = 128$, 3(*C*H$_3$)], 30.7 [q, $^1J_{C-H} = 126$, 3(C(*C*H$_3$)$_3$)], 32.0 [s, 3(*C*(CH$_3$)$_3$)], 103.2 [d, $^1J_{C-H} = 174$, 3(*C*$_3$N$_2$H) (1C)], 117.0 [d, $^1J_{C-H} = 146$, *C*$_6$H$_4$ (2C)], 121.5 [d, $^1J_{C-H} = 158$, *C*$_6$H$_4$ (2C)], 136.2 [s, *C*$_6$H$_4$ (para C)], 144.2 [s, 3(*C*$_3$N$_2$H) (1C)], 158.2 [s, *C*$_6$H$_4$ (ipso C)], 163.9 [s, 3(*C*$_3$N$_2$H) (1C)]. IR (KBr, cm^{-1}): 3416 (w) [ν(N−H)], 3345 (w) [ν(N−H)], 2962 (s), 2551 (w) [ν(B−H)], 1609 (m), 1542 (s), 1507 (vs), 1433 (s), 1365 (s), 1342 (m), 1304 (vs), 1250 (s), 1187 (vs), 1069 (s), 1032 (m), 988 (w), 830 (s), 794 (s), 767 (s), 732 (m), 696 (m), 651 (s), 519 (m).

Synthesis of [Tp$^{Bu^t,Me}$]ZnOC$_6$H$_4$OMe. A solution of 4-methoxyphenol (56 mg, 0.45 mmol) and [Tp$^{Bu^t,Me}$]ZnH (200 mg, 0.41 mmol) in benzene (10 mL) was heated at 120 °C for 2 days. The reaction mixture was filtered, and the filtrate was lyophilized giving [Tp$^{Bu^t,Me}$]-ZnOC$_6$H$_4$OMe as a white solid (206 mg, 82%). Anal. Calcd for $C_{31}H_{47}$-BN_6O_2Zn: C, 60.8; H, 7.7; N, 13.7. Found: C, 60.7; H, 7.7; N 13.1. ^{1}H NMR (C_6D_6): 1.49 [s, 3(C(C*H*$_3$)$_3$)], 2.08 [s, 3(C*H*$_3$)], 3.58, [s, (OC*H*$_3$)], 5.63 [s, 3(C$_3$N$_2$*H*)], 7.10 [d, $^3J_{H-H} = 9$, C$_6$*H*$_4$ (2H)], 7.28 [d, $^3J_{H-H} = 9$, C$_6$*H*$_4$ (2H)], *H*B not observed. ^{13}C NMR (C_6D_6): 12.6 [q, $^1J_{C-H} = 128$, 3(*C*H$_3$)], 30.7 [q, $^1J_{C-H} = 126$, 3(C(*C*H$_3$)$_3$)], 32.0 [s, 3(*C*(CH$_3$)$_3$)], 55.6 [q, $^1J_{C-H} = 142$, O*C*H$_3$], 103.2 [d, $^1J_{C-H} = 171$, 3(*C*$_3$N$_2$H) (1C)], 115.0 [dd, $^1J_{C-H} = 156$, $^2J_{C-H} = 6$, *C*$_6$H$_4$ (2C)], 121.5 [dd, $^1J_{C-H} = 150$, $^2J_{C-H} = 6$, *C*$_6$H$_4$ (2C)], 144.2 [s, 3(*C*$_3$N$_2$H) (1C)], 151.0 [s, *C*$_6$H$_4$ (para C)], 159.4 [s, *C*$_6$H$_4$ (ipso C)], 163.9 [s, 3(*C*$_3$N$_2$H) (1C)]. IR (KBr, cm^{-1}): 2961 (s), 2829 (w), 2554 (w) [ν(B−H)], 1542 (s), 1503 (vs), 1464 (s), 1436 (s), 1385 (m), 1366 (s), 1343 (m), 1302 (s), 1263 (s), 1231 (vs), 1186 (vs), 1126 (w), 1097 (w), 1068 (s), 1033 (m), 985 (w), 857 (w), 827 (s), 789 (s), 765 (vs), 732 (w), 680 (w), 646 (s), 521 (w).

Synthesis of [Tp$^{Bu^t,Me}$]ZnOC$_6$H$_4$Bu^t. A solution of 4-*tert*-butylphenol (21 mg, 0.14 mmol) and [Tp$^{Bu^t,Me}$]ZnH (70 mg, 0.14 mmol) in benzene (3.5 mL) was heated at 120 °C for 3 days and then lyophilized to give [Tp$^{Bu^t,Me}$]ZnOC$_6$H$_4$Bu^t as a white solid (57 mg, 73%). Anal.

(23) Kitajima, N.; Tolman, W. B. *Prog. Inorg. Chem.* **1995**, *43*, 419−531.

(24) In support of this statement, the ionization potential of the fragment {[Tp$^{Bu^t,Me}$]Zn} is calculated to be 20.0 kcal mol^{-1} lower than that for {[Tp]Zn}.

(25) Ramaswamy, S.; Park, D.-H.; Plapp, B. V. *Biochemistry* **1999**, *38*, 13951−13959.

(26) dipicH$_2$ = pyridine-2,6-dicarboxylic acid.

(27) Thorn, D. L.; Harlow, R. L.; Herron, N. *Inorg. Chem.* **1996**, *35*, 547−548.

(28) (a) McNally, J. P.; Leong, V. S.; Cooper, N. J. In *Experimental Organometallic Chemistry*; Wayda, A. L., Darensbourg, M. Y., Eds.; American Chemical Society: Washington, DC, 1987; Chapter 2, pp 6−23. (b) Burger, B. J.; Bercaw, J. E. In *Experimental Organometallic Chemistry*; Wayda, A. L., Darensbourg, M. Y., Eds.; American Chemical Society: Washington, DC, 1987; Chapter 4, pp 79−98. (c) Shriver, D. F.; Drezdzon, M. A. *The Manipulation of Air-Sensitive Compounds*, 2nd ed.; Wiley-Interscience: New York, 1986.

Calcd for $C_{34}H_{53}BN_6OZn$: C, 64.0; H, 8.4; N, 13.2. Found: C, 64.1; H, 8.6; N 12.6. ^{1}H NMR (C_6D_6): 1.45 [s, (C_6H_4)C(CH_3)$_3$], 1.50 [s, 3(C(CH_3)$_3$)], 2.08 [s, 3(CH_3)], 5.63 [s, 3(C_3N_2H)], 7.33 [d, $^3J_{H-H}$ = 9, C_6H_4 (2H)], 7.50 [d, $^3J_{H-H}$ = 9, C_6H_4 (2H)], *H*B not observed. ^{13}C NMR (C_6D_6): 12.6 [q, $^1J_{C-H}$ = 128, 3(*C*H$_3$)], 30.7 [q, $^1J_{C-H}$ = 124, 3(C(*C*H$_3$)$_3$)], 32.0 [s, 3(*C*(CH$_3$)$_3$)], 32.2 [q, $^1J_{C-H}$ = 122, (C_6H_4)C-(*C*H$_3$)$_3$], 34.0 [s, (C_6H_4)*C*(CH$_3$)$_3$], 103.2 [d, $^1J_{C-H}$ = 171, 3(*C*$_3$N$_2$H) (1C)], 120.9 [dd, $^1J_{C-H}$ = 155, $^2J_{C-H}$ = 5, C_6H_4 (2C)], 126.0 [dd, $^1J_{C-H}$ = 152, $^2J_{C-H}$ = 8, C_6H_4 (2C)], 137.5 [s, C_6H_4 (para C)], 144.2 [s, 3(*C*$_3$N$_2$H) (1C)], 162.7 [s, C_6H_4 (ipso C)], 163.9 [s, 3(*C*$_3$N$_2$H) (1C)]. IR (KBr, cm^{-1}): 2922 (vs), 2855 (vs), 2547 (w) [ν(B−H)], 1605 (m), 1542 (m), 1511 (s), 1465 (s), 1365 (s), 1340 (w), 1315 (s), 1263 (w), 1248 (w), 1187 (s), 1107 (w), 1068 (s), 1028 (m), 988 (w), 878 (w), 811 (w), 858 (w), 829 (m), 811 (m), 792 (m), 767 (m), 730 (w), 694 (w), 681 (w), 646 (w), 551 (w), 521 (w).

Synthesis of [Tp^{But,Me}]ZnOC$_6$H$_4$Me. *p*-Cresol was purified before use by storing a solution in benzene over molecular sieves for 2 days, followed by filtration and removal of the solvent in vacuo. A solution of *p*-cresol (52 mg, 0.48 mmol) and [Tp^{But,Me}]ZnH (200 mg, 0.41 mmol) in benzene (10 mL) was heated at 120 °C for 1.5 days. The reaction mixture was filtered, and the filtrate was lyophilized to give [Tp^{But,Me}]ZnOC$_6$H$_4$Me as a white solid (149 mg, 61%). Anal. Calcd for $C_{31}H_{47}BN_6OZn$: C, 62.5; H, 7.9; N, 14.1. Found: C, 62.2; H, 7.9; N 15.0. ^{1}H NMR (C_6D_6): 1.49 [s, 3(C(CH_3)$_3$)], 2.08 [s, 3(CH_3)], 2.40 [s, (C_6H_4)CH_3], 5.63 [s, 3(C_3N_2H)], 7.29 [m, C_6H_4], *H*B not observed. ^{13}C NMR (C_6D_6): 12.6 [q, $^1J_{C-H}$ = 128, 3(*C*H$_3$)], 20.9 [q, $^1J_{C-H}$ = 125, (C_6H_4)*C*H$_3$], 30.7 [q, $^1J_{C-H}$ = 126, 3(C(*C*H$_3$)$_3$)], 32.0 [s, 3(*C*(CH$_3$)$_3$)], 103.2 [d, $^1J_{C-H}$ = 174, 3(*C*$_3$N$_2$H) (1C)], 121.4 [d, $^1J_{C-H}$ = 154, C_6H_4 (2C)], 123.8 [s, C_6H_4 (para C)], 129.9 [d, $^1J_{C-H}$ = 152, C_6H_4 (2C)], 144.3 [s, 3(*C*$_3$N$_2$H) (1C)], 162.9 [s, C_6H_4 (ipso C)], 164.0 [s, 3(*C*$_3$N$_2$H) (1C)]. IR (KBr, cm^{-1}): 2963 (s), 2553, (w) [ν(B−H)], 1609 (s), 1544 (s), 1509 (vs), 1477 (s), 1434 (s), 1366 (s), 1341 (m), 1305 (vs), 1246 (m), 1188 (vs), 1128 (w), 1103 (w), 1068 (s), 1030 (m), 987 (w), 869 (w), 824 (s), 789 (s), 769 (s), 680 (w), 648 (m), 517 (m).

Synthesis of [Tp^{But,Me}]ZnOC$_6$H$_5$. A solution of phenol (31 mg, 0.33 mmol) and [Tp^{But,Me}]ZnH (150 mg, 0.31 mmol) in benzene (5 mL) was heated at 120 °C for 1.5 days. The reaction mixture was filtered, and the filtrate was lyophilized to give [Tp^{But,Me}]ZnOC$_6$H$_5$ as a white solid (95 mg, 53%). Anal. Calcd for $C_{30}H_{45}BN_6OZn$: C, 61.9; H, 7.8; N, 14.4. Found: C, 62.2; H, 7.8; N 14.2. ^{1}H NMR (C_6D_6): 1.47 [s, 3(C(CH_3)$_3$)], 2.07 [s, 3(CH_3)], 5.62 [s, 3(C_3N_2H)], 6.95 [tt, $^3J_{H-H}$ = 7, $^4J_{H-H}$ = 1, C_6H_5 (1H)], 7.37 [m, C_6H_5 (2H)], 7.48 [m, C_6H_5 (2H)], *H*B not observed. ^{13}C NMR (C_6D_6): 12.6 [q, $^1J_{C-H}$ = 128, 3(*C*H$_3$)], 30.7 [q, $^1J_{C-H}$ = 126, 3(C(*C*H$_3$)$_3$)], 32.0 [s, 3(*C*(CH$_3$)$_3$)], 103.2 [d, $^1J_{C-H}$ = 171, 3(*C*$_3$N$_2$H) (1C)], 115.8 [d, $^1J_{C-H}$ = 158, C_6H_4 (para C)], 121.8 [dt, $^1J_{C-H}$ = 152, $^2J_{C-H}$ = 7, C_6H_5 (2C)], 129.4 [dd, $^1J_{C-H}$ = 155, $^2J_{C-H}$ = 9, C_6H_4 (2C)], 144.3 [s, 3(*C*$_3$N$_2$H) (1C)], 164.0 [s, 3(*C*$_3$N$_2$H) (1C)], 165.2 [s, C_6H_4 (ipso C)]. IR (KBr, cm^{-1}): 2968 (s), 2551 (w) [ν(B−H)], 1590 (s), 1544 (s), 1495 (vs), 1435 (s), 1365 (s), 1343 (m), 1303 (vs), 1246 (m), 1188 (vs), 1069 (s), 1030 (m), 995 (w), 859 (m), 790 (s), 768 (s), 757 (s), 695 (m), 648 (m), 520 (w).

Synthesis of [Tp^{But,Me}]ZnOC$_6$H$_4$I. A solution of 4-iodophenol (74 mg, 0.34 mmol) and [Tp^{But,Me}]ZnH (100 mg, 0.20 mmol) in benzene (10 mL) was heated at 120 °C for 1.5 days. The reaction mixture was filtered, and the filtrate was lyophilized to give [Tp^{But,Me}]ZnOC$_6$H$_4$I as a white solid (90 mg, 64%). Anal. Calcd for $C_{30}H_{44}BIN_6OZn$: C, 50.9; H, 6.3; N, 11.9. Found: C, 50.8; H, 6.2; N 11.4. ^{1}H NMR (C_6D_6): 1.40 [s, 3(C(CH_3)$_3$)], 2.06 [s, 3(CH_3)], 5.61 [s, 3(C_3N_2H)], 7.03 [d, $^3J_{H-H}$ = 9, C_6H_4 (2H)], 7.70 [d, $^3J_{H-H}$ = 9, C_6H_4 (2H)], *H*B not observed. ^{13}C NMR (C_6D_6): 12.6 [q, $^1J_{C-H}$ = 128, 3(*C*H$_3$)], 30.6 [q, $^1J_{C-H}$ = 126, 3(C(*C*H$_3$)$_3$)], 31.9 [s, 3(*C*(CH$_3$)$_3$)], 76.2 [s, C_6H_4 (para C)], 103.3 [d, $^1J_{C-H}$ = 174, 3(*C*$_3$N$_2$H) (1C)], 124.4 [dd, $^1J_{C-H}$ = 162, $^2J_{C-H}$ = 5, C_6H_4 (2C)], 138.2 [dd, $^1J_{C-H}$ = 161, $^2J_{C-H}$ = 7, C_6H_4 (2C)], 144.4 [s, 3(*C*$_3$N$_2$H) (1C)], 163.9 [s, 3(*C*$_3$N$_2$H) (1C)], 164.9 [s, C_6H_4 (ipso C)]. IR (KBr, cm^{-1}): 2961 (s), 2557 (w) [ν(B−H)], 1576 (s), 1541 (s), 1485 (vs), 1433 (s), 1384 (m), 1365 (s), 1342 (m), 1307 (vs), 1246 (m), 1186 (vs), 1068 (s), 1032 (m), 986 (w), 857 (m), 825 (s), 787 (s), 766 (s), 680 (w), 645 (s), 521 (w).

Synthesis of [Tp^{But,Me}]ZnOC$_6$H$_4$CO$_2$Me. A solution of 4-hydroxymethylbenzoate (31 mg, 0.20 mmol) and [Tp^{But,Me}]ZnH (100 mg, 0.20 mmol) in benzene (5 mL) was heated at 120 °C for 2 days and then lyophilized to give [Tp^{But,Me}]ZnOC$_6$H$_4$CO$_2$Me as a white solid (79 mg, 62%). Anal. Calcd for $C_{32}H_{47}BN_6O_3Zn$: C, 60.1; H, 7.4; N, 13.1. Found: C, 60.3; H, 7.2; N 13.3. ^{1}H NMR (C_6D_6): 1.40 [s, 3(C(CH_3)$_3$)], 2.06 [s, 3(CH_3)], 3.64 [s, OCH_3], 5.61 [s, 3(C_3N_2H)], 7.29 [d, $^3J_{H-H}$ = 9, C_6H_4 (2H)], 8.51 [d, $^3J_{H-H}$ = 9, C_6H_4 (2H)], *H*B not observed. ^{13}C NMR (C_6D_6): 12.6 [q, $^1J_{C-H}$ = 128, 3(*C*H$_3$)], 30.6 [q, $^1J_{C-H}$ = 126, 3(C(*C*H$_3$)$_3$)], 31.9 [s, 3(*C*(CH$_3$)$_3$)], 51.0 [q, $^1J_{C-H}$ = 146, CO$_2$*C*H$_3$], 103.3 [d, $^1J_{C-H}$ = 174, 3(*C*$_3$N$_2$H) (1C)], 118.1 [s, C_6H_4 (para C)], 121.3 [dd, $^1J_{C-H}$ = 157, $^2J_{C-H}$ = 4, C_6H_4 (2C)], 132.2 [dd, $^1J_{C-H}$ = 159, $^2J_{C-H}$ = 7, C_6H_4 (2C)], 144.5 [s, 3(*C*$_3$N$_2$H) (1C)], 163.9 [s, 3(*C*$_3$N$_2$H) (1C)], 167.6 [s, C_6H_4 (ipso C)], 169.9 [s, *C*O$_2$CH$_3$]. IR (KBr, cm^{-1}): 2965 (s), 2871 (m), 2560 (w) [ν(B−H)], 1712 (s) [ν(CO)], 1597 (vs), 1544 (s), 1513 (s), 1476 (m), 1433 (s), 1366 (m), 1331 (vs), 1276 (vs), 1189 (s), 1159 (s), 1111 (m), 1096 (m), 1068 (m), 1030 (w), 988 (w), 852 (w), 796 (w), 772 (m), 705 (w), 680 (w), 655 (w), 520 (w), 455 (w).

Synthesis of [Tp^{But,Me}]ZnOC$_6$H$_4$COMe. A solution of 4-hydroxyacetophenone (61 mg, 0.45 mmol) and [Tp^{But,Me}]ZnH (200 mg, 0.41 mmol) in benzene (10 mL) was heated at 120 °C for 2 days. The reaction mixture was filtered, and the filtrate was lyophilized to give [Tp^{But,Me}]ZnOC$_6$H$_4$COMe as a white solid (182 mg, 71%). Anal. Calcd for $C_{32}H_{47}BN_6O_2Zn$: C, 61.6; H, 7.6; N, 13.5. Found: C, 61.7; H, 7.8; N 13.0. ^{1}H NMR (C_6D_6): 1.42 [s, 3(C(CH_3)$_3$)], 2.06 [s, 3(CH_3)], 2.37 [s, COCH_3], 5.61 [s, 3(C_3N_2H)], 7.24 [d, $^3J_{H-H}$ = 9, C_6H_4 (2H)], 8.22 [d, $^3J_{H-H}$ = 9, C_6H_4 (2H)], *H*B not observed. ^{13}C NMR (C_6D_6): 12.6 [q, $^1J_{C-H}$ = 128, 3(*C*H$_3$)], 25.9 [q, $^1J_{C-H}$ = 126, CO*C*H$_3$], 30.6 [q, $^1J_{C-H}$ = 126, 3(C(*C*H$_3$)$_3$)], 31.9 [s, 3(*C*(CH$_3$)$_3$)], 103.3 [d, $^1J_{C-H}$ = 174, 3(*C*$_3$N$_2$H) (1C)], 121.1 [dd, $^1J_{C-H}$ = 157, $^2J_{C-H}$ = 4, C_6H_4 (2C)], 126.8 [s, C_6H_4 (para C)], 131.2 [dd, $^1J_{C-H}$ = 156, $^2J_{C-H}$ = 7, C_6H_4 (2C)], 144.6 [s, 3(*C*$_3$N$_2$H) (1C)], 163.9 [s, 3(*C*$_3$N$_2$H) (1C)], 170.0 [s, C_6H_4 (ipso C)], 195.0 [s, *C*OCH$_3$]. IR (KBr, cm^{-1}): 2960 (s), 2553 (w) [ν-(BH)], 1668 (s) [ν(CO)], 1587 (vs), 1544 (s), 1515 (s), 1466 (m), 1424 (s), 1336 (vs), 1274 (vs), 1188 (vs), 1163 (s), 1067 (s), 1031 (m), 952 (w), 873 (m), 838 (s), 795 (s), 767 (s), 719 (w), 679 (w), 650 (m), 586 (s), 521 (w).

Synthesis of [Tp^{But,Me}]ZnOC$_6$H$_4$NO$_2$. A solution of 4-nitrophenol (64 mg, 0.46 mmol) and [Tp^{But,Me}]ZnH (200 mg, 0.41 mmol) in benzene (5 mL) was heated at 120 °C for 1 day. The reaction mixture was filtered, and the filtrate was lyophilized to give [Tp^{But,Me}]ZnOC$_6$H$_4$-NO$_2$ as a yellow solid (149 mg, 58%). Anal. Calcd for $C_{30}H_{44}BN_7O_3$-Zn: C, 57.5; H, 7.1; N, 15.6. Found: C, 57.8; H, 6.9; N, 15.7. ^{1}H NMR (C_6D_6): 1.35 [s, 3(C(CH_3)$_3$)], 2.06 [s, 3(CH_3)], 5.61 [s, 3(C_3N_2H)], 7.02 [d, $^3J_{H-H}$ = 9, C_6H_4 (2H)], 8.41 [d, $^3J_{H-H}$ = 9, C_6H_4 (2H)], *H*B not observed. ^{13}C NMR (C_6D_6): 12.6 [q, $^1J_{C-H}$ = 128, 3(*C*H$_3$)], 30.5 [q, $^1J_{C-H}$ = 126, 3(C(*C*H$_3$)$_3$)], 31.9 [s, 3(*C*(CH$_3$)$_3$)], 103.4 [d, $^1J_{C-H}$ = 174, 3(*C*$_3$N$_2$H) (1C)], 120.8 [dd, $^1J_{C-H}$ = 160, $^2J_{C-H}$ = 5, C_6H_4 (2C)], 126.5 [dd, $^1J_{C-H}$ = 162, $^2J_{C-H}$ = 5, C_6H_4 (2C)], 138.2 [s, C_6H_4 (para C)], 144.8 [s, 3(*C*$_3$N$_2$H) (1C)], 163.8 [s, 3(*C*$_3$N$_2$H) (1C)], 171.4 [s, C_6H_4 (ipso C)]. IR (KBr, cm^{-1}): 2965 (s), 2555 (w) [ν(BH)], 1585 (vs), 1543 (s), 1503 (vs), 1428 (s), 1366 (s), 1320 (vs), 1247 (m), 1187 (s), 1111 (s), 1069 (s), 1032 (m), 989 (w), 872 (m), 848 (m), 793 (s), 768 (s), 681 (m), 667 (s), 649 (m), 523 (w).

Measurement of the Equilibrium Constant for Alcoholysis of [Tp^{But,Me}]ZnOH with *p*-Cresol. A solution of [Tp^{But,Me}]ZnOC$_6$H$_4$Me (9.3 mg, 0.016 mmol) in THF-d_8 (600 μL) was treated with 12 5-μL portions of a solution of D_2O in THF-d_8 (6.37 M). After each addition, the solution was allowed to equilibrate for at least 5 min and the concentration ratio of [Tp^{But,Me}]ZnOC$_6$H$_4$Me/[Tp^{But,Me}]ZnOH was determined by ^{1}H NMR spectroscopy. The equilibrium constant K_{p-Me} = [{[Tp^{But,Me}]ZnOC$_6$H$_4$Me}][H$_2$O]/[{[Tp^{But,Me}]ZnOH}][*p*-XC$_6$H$_4$OH] was obtained by computer fitting of the data. The experiment was repeated three times, and an average value of the equilibrium constant was obtained.

Measurement of the Equilibrium Constant for Alcohol Exchange of [Tp^{But,Me}]ZnOC$_6$H$_4$Me with ArOH. A solution was prepared of ~10 mg of [Tp^{But,Me}]ZnOC$_6$H$_4$X, (X = OMe, Bu^t, H, I, CO$_2$Me, COMe, NO$_2$) and *p*-cresol (~2 mg) in C_6D_6. The concentration ratios of [Tp^{But,Me}]ZnOC$_6$H$_4$Me/[Tp^{But,Me}]ZnOC$_6$H$_4$X and HOC$_6$H$_4$X/HOC$_6$H$_4$Me were obtained by ^{1}H NMR spectroscopy. The relative concentrations were varied, and six to eight independent measurements were made

Table 5. Crystal, Intensity Collection, and Refinement Data

	$[Tp^{Bu^t,Me}]ZnOC_6H_4C(O)Me$	$[Tp^{Bu^t,Me}]ZnOC_6H_4NO_2 \cdot C_6H_6$	$[Tp^{Bu^t,Me}]ZnOC_6H_4NH_2$	$[Tp^{Bu^t,Me}]ZnOC_6H_4Bu^t$
lattice	monoclinic	monoclinic	monoclinic	monoclinic
formula	$C_{32}H_{47}BN_6O_2Zn$	$C_{36}H_{50}BN_7O_3Zn$	$C_{30}H_{46}BN_7OZn$	$C_{34}H_{53}BN_6OZn$
formula wt	623.94	705.01	596.92	638.00
space group	$P2_1/c$ (No. 14)	$P2_1$ (No. 4)	$P2_1/n$ (No. 14)	$P2_1/c$ (No. 14)
a/Å	11.0272(7)	11.912(6)	21.9967(12)	21.9346(11)
b/Å	14.7628(9)	11.194(5)	15.4016(7)	18.9262(9)
c/Å	22.756(2)	14.893(7)	22.1563(11)	18.4830(9)
α/deg	90	90	90	90
β/deg	114.180(1)	106.766(8)	119.396(1)	107.275(1)
γ/deg	90	90	90	90
V/Å^3	3379.4(4)	1901(1)	6539.8(6)	7326.9(6)
Z	4	2	8	8
temp/K	213	233	223	203
μ (Mo Kα)/mm^{-1}	0.763	0.689	0.784	0.703
no. of data	7547	8231	15117	16595
no. of params	396	435	770	814
R_1	0.0346	0.0484	0.0555	0.0651
wR_2	0.0844	0.1110	0.1059	0.1149

for each substituent to give an average value for the equilibrium constant, $K_{exch} = [\{[Tp^{Bu^t,Me}]ZnOC_6H_4Me\}][p\text{-}XC_6H_4OH]/[\{[Tp^{Bu^t,Me}]ZnOC_6H_4X\}][p\text{-}MeC_6H_4OH]$. The equilibrium constants for the reaction between $[Tp^{Bu^t,Me}]ZnOH$ and $p\text{-}XC_6H_4OH$ were determined by the expression $K_{p-X} = K_{p-Me}/K_{exch}$. ΔH values for the reactions of $[Tp^{Bu^t,Me}]ZnOH$ with XC_6H_4OH are estimated from the experimental ΔG values using the assumption that $\Delta S \approx 0$, an approximation that was confirmed for the reaction of $[Tp^{Bu^t,Me}]ZnOH$ with MeC_6H_4OH ($\Delta H = -1.3(1)$ kcal mol^{-1}, $\Delta S = -0.3(2)$ eu over the range 250−330 K). The enthalpies for X = OMe, Bu^t, Me, H, I, CO_2Me, and C(O)Me have also been determined by titration calorimetry. These values are in reasonable agreement with those determined by the equilibrium studies, but are ∼1−4 kcal mol^{-1} more exothermic. However, the calorimetry values were not averaged over many experiments and so are considered to be less reliable than those obtained by the equilibrium study.

X-ray Structure Determinations. X-ray diffraction data for $[Tp^{Bu^t,Me}]ZnOC_6H_4X$ (X = Bu^t, C(O)Me, NH_2, NO_2) were collected on a Bruker P4 diffractometer equipped with a SMART CCD detector. Crystal data, data collection, and refinement parameters are summarized in Table 5. The structures were solved using direct methods and standard difference map techniques and were refined by full-matrix least-squares procedures on F^2 with SHELXTL (Version 5.03).[29] Hydrogen atoms on carbon were included in calculated positions.

Computational Details. All calculations were performed using Jaguar.[9] Initial geometries were obtained from crystal structures where available, and in other cases, the desired molecule was built through modification of the coordinates of a similar compound with known structure. DFT geometry optimizations were performed on all complexes at the B3LYP level using the LACVP** basis set. Single-point energies were calculated for the optimized structures at the B3LYP level using the triple ζ basis set CC-PVTZ (-f) for all elements except boron, for which the 6-31G** basis set was used, and zinc and iodine, for which the LACV3P** basis set was used.

Conclusion

In summary, the present study indicates the extent to which the thermodynamics of the formation of a zinc alkoxide derivative from a hydroxide complex is influenced by the nature of the alcohol and ligands attached to zinc. Thus, zinc alkoxide formation is favored electronically by incorporation of electron-withdrawing substituents in the alcohol but is disfavored sterically for bulky alcohols. Furthermore, alkoxide formation is more favored for [Tp]ZnOR derivatives than for their $[Tp^{Bu^t,Me}]ZnOR$ counterparts. These trends are a result of homolytic Zn−OR BDEs being more sensitive to the nature of R than are the corresponding H−OR bond energies. Thus, electron-withdrawing substituents increase Zn−OAR bond energies to a greater extent than H−OAr bond energies, while bulky substituents decrease Zn−OR bond energies to a greater extent than H−OR bond energies. The trends reported for this zinc system are of relevance to the tetrahedral zinc alkoxide intermediate in the catalytic cycle of liver alcohol dehydrogenase—such information is of importance since other systems, e.g., (dipic)VO(OR),[27] exhibit a trend opposite to that reported here. With the exception of derivatives of acidic alcohols (e.g., nitrophenol), the zinc alkoxide complexes $[Tp^{RR'}]ZnOR$ are very unstable toward hydrolysis. This hydrolytic instability of simple zinc alkoxide complexes suggests that the active site environment of LADH plays an important role in stabilizing the alkoxide intermediate, possibly via hydrogen-bonding interactions. Future studies are intended to investigate the influence of substituents on another step of the catalytic cycle, namely, hydride transfer from the alkoxide.

Acknowledgment. We thank the National Institutes of Health (GM46502 to G.P. and GM40526 to R.A.F.) for support of this research, Professor Ronald Breslow for the use of his titration calorimeter, and Professor Sally Chapman and Dr. Barry Dunietz for helpful discussions.

Supporting Information Available: Tables of crystallographic data (PDF). This material is available free of charge via the Internet at http://pubs.acs.org.

JA002286D

(29) Sheldrick, G. M. SHELXTL, An Integrated System for Solving, Refining and Displaying Crystal Structures from Diffration Data. University of Göttingen, Göttingen, Federal Republic of Germany, 1981.